Chemical Engineering Journal Advances 7 (2021) 100122

Contents lists available at ScienceDirect

Chemical Engineering Journal Advances

journal homepage: www.elsevier.com/locate/ceja

An environmentally friendly method for efficient atmospheric oxidation of pyrrhotite in arsenopyrite/pyrite calcine

Lin Li[a,b], Jingxiu Wang[a], Chengqian Wu[a], Ahmad Ghahreman[a,*]

[a] Hydrometallurgy and Environment Laboratory, The Robert M. Buchan Department of Mining, Queen's University, 25 Union St., Kingston, ON K7L 3N6, Canada
[b] National Research Council Canada, Ottawa, ON K1A 0R6, Canada

ARTICLE INFO

Keywords:
Calcine
Oxidation
Pyrrhotite
Thermal phase transformation
Sulfur balance
Pyrolysis

ABSTRACT

Pyrite and arsenopyrite are the most common hosts for invisible gold, but pyrite and arsenic are refractory during conventional sulfide oxidation, which significantly challenges subsequent gold extraction. One option is high-temperature pretreatment of arsenical materials to sequester > 90% of the arsenic as a gas, then convert it to a stable form. This process produces a calcine similar in composition to pyrrhotite ($Fe_{1-x}S$) but with higher porosity. In this study, the calcine product is oxidized with an efficient, cost-effective atmospheric process using acidic and near-neutral solutions. A sulfur mass balance analysis method based on iron sulfide thermal transformation in nitrogen atmosphere was developed to quantify the oxidation efficiency of pyrrhotite leaching. The optimization confirmed that > 90% of the calcine was oxidized by Fe^{3+} (5 and 10 g/L) and O_2 (0.5 L/min) at pH 1 after 48 h and at 95 °C even without ultrafine grinding. Elemental sulfur was the main oxidation product when the oxidation pH was 1,2. This study provides the foundation for the development of a low-cost and environmentally friendly process option for pretreatment of arsenical sulfide refractory gold materials.

1. Introduction

Gold extraction from refractory sulfide ores has attracted recent interest from mining companies because there is significant potential to exploit "invisible" gold (i.e., finely disseminated Au particles < 1 μm in size) in common sulfide minerals such as pyrite and arsenopyrite [4,25]. Efficient pyrite and arsenopyrite oxidation is essential to permit subsequent cyanide leaching to extract this gold. As a refractory sulfide mineral, pyrite has been the subject of many hydrometallurgical studies of its oxidation behavior (e.g., [7,23,31]). Further, numerous environmental science studies have focused on geochemical oxidation of pyrite as the main source for acid mine drainage (e.g., [13,24,33]).

There have been many methods to remove As from arsenopyrite, including roasting, chlorination, pressure oxidation, chemical and bacterial leaching [19]. Roasting is the most attractive technology due to the adaptivity, easy operation, low cost, and reliability. Two-stage roasting is the conventional industrial treatment for refractory arsenopyrite Eq. (1). The first stage is a de-arsenification process to transform arsenic into gas phase under lower temperature (450 °C to 550 °C) in an oxygen-deficient atmosphere, producing a sulfide calcine with low arsenic content similar to pyrrhotite ($Fe_{1-x}S$, x = 0–0.2) for further processing [11]. The calcined product is generally porous and spongy. The second stage relates to oxidation of calcine to Fe_2O_3 and SO_2 in surplus oxygen conditions at higher temperature (600 °C to 700 °C) for a highly porous product.

$$2FeAsS\ (s) + 5O_2 \rightarrow Fe_2O_3(s) + As_2O_3(g) + 2SO_2(g) \quad (1)$$

Two-step roasting has high capital and operating costs and the As_2O_3 and SO_2 emissions cause environmental problems [1,28]. Arsenopyrite pyrolysis in an inert environment containing N_2 or CO_2 was a suitable alternative to two-stage roasting to prevent gaseous SO_2 emissions [12]. However, gold recovery from cyanidation of the pyrolysis products (mainly pyrrhotite) was < 50%: significant amounts of gold remained in the calcine as a solid solution. Calcine is refractory: its direct cyanidation often results in low gold recovery.

Unlike pyrite, research on pyrrhotite oxidation is scarce, and the oxidation mechanism is poorly understood. Pyrrhotite chemistry can be complicated due to the uncertainty of the Fe/S ratio: the x in $Fe_{1-x}S$ can range from nearly 0 (FeS) to 0.125 (Fe_7S_8). The extent of iron deficiency in the crystal structure can affect pyrrhotite oxidation [29], though how it is affected has not been conclusively quantified [22]. Controversy regarding the mechanism of pyrrhotite oxidation encompasses the intermediate and final oxidation products and reaction routes [16]. Pyrrhotite oxidation by either O_2 or Fe^{3+}—the most common oxidants for sulfide mineral oxidation—can produce sulfate and elemental sulfur (S^0), depending on the availability of H^+, and involve polysulfide and iron-deficient sulfide intermediates [8]. Eqs. 2 and 3 describe the main reactions when O_2 is the primary oxidant at near-alkaline conditions.

* Corresponding author.
E-mail address: ahmad.g@queensu.ca (A. Ghahreman).

https://doi.org/10.1016/j.ceja.2021.100122
Received 2 February 2021; Received in revised form 1 May 2021; Accepted 4 May 2021

Table 1
Comparison of conventional pyrrhotite oxidation process.

Method	Conditions and results	Merits	Drawbacks	Ref.
Mechanical activation	Mechanically active for 10-40 min, the leaching recovery of Fe is 10–30 times more.	1. Accelerated reaction rate; 2. Reduced leaching temperature	1.Agglomereation of fine particles; 2. Relatively low energy efficiency	[34]
Acid pressure oxidation	At 80-110 °C, pyrrhotite oxidation fast in 2 h and significantly slow down. At 130-180 °C, the pressure oxidation was totally inhibited due to molten sulphur.	High initial oxidation rate	1. High capital cost, 2. Not completed oxidation.	[14]
Hot nitric acid leaching	At 95 °C, 93% of pyrrhotite was oxidized after 150 min.	1. Rapidly reaction rate; 2. Atmospheric condition.	1. NO and NO_2 gas formation 2. Expensive lixiviate agents; 3. Customized reaction equipment	([10]

At low pH, oxidation may occur as given in Eqs. 4 and 5 since Fe^{3+} is a stronger oxidant than O_2 in acids [29].

$$Fe_{1-x}S\ (s)\ +\left(2-\frac{x}{2}\right)O_2+xH_2O\rightarrow(1-x)Fe^{2+}\ +\ SO_4^{2-}+2xH^+ \quad (2)$$

$$Fe_{1-x}S\ (s)\ +\left(2-\frac{x}{2}\right)O_2+2(1-x)H^+\rightarrow(1-x)Fe^{2+}\ +\ S^0+(1-x)H_2O \quad (3)$$

$$Fe_{1-x}S\ (s)\ +(8-2x)Fe^{3+}+4H_2O\rightarrow(9-3x)Fe^{2+}\ +\ SO_4^{2-}+8H^+ \quad (4)$$

$$Fe_{1-x}S\ (s)\ +(2-2x)Fe^{3+}\rightarrow(3-3x)Fe^{2+}\ +\ S^0(s) \quad (5)$$

Previous studies have investigated atmospheric oxidative leaching of pyrrhotite in terms of incomplete oxidation, oxidation products, and metastable intermediates such as thiosulfate, polythionate, and $S_4O_6^{2-}$ [26, 27], yet few have addressed the effect of pH on pyrrhotite oxidation. Pyrrhotite oxidation by $Fe^{3+}$and O_2 can be either acid-generating Eqs. 2,(3) or -consuming Eqs. 4,(5), reflecting the complex nature of pyrrhotite oxidation. Therefore, pH is a crucial factor when designing a pyrrhotite oxidative leaching system. Effective pH control can prevent precipitation of Fe^{3+}.

Although pyrrhotite is highly reactive [3], the oxidative leaching efficiency of natural pyrrhotite can be low due to extensive passivation arising from S^0 deposition on the surfaces of partially oxidized pyrrhotite minerals. Mechanical activation [34], acid pressure oxidation [14], and hot nitric acid oxidation [10] have been shown to inhibit passivation, but mechanical activation and acid pressure oxidation are associated with high operating costs, and the hot nitric acid process requires customized reaction equipment (Table 1). High-pressure oxidation also has to deal with a molten sulfur product that passivates partially oxidized minerals. In view of all these shortcomings, it is thus necessary and noteworthy to find a viable method to leach pyrrhotite effectively to liberate invisible gold from the pyrrhotite lattice prior to cyanidation. In this study, we propose a viable hydrometallurgical process to fully oxidize calcine with O_2 and Fe^{3+} as oxidants at 95°C and atmospheric pressure environmentally friendly and economically.

Calcined pyrrhotite could have different oxidation kinetics than natural pyrrhotite. The loss of As and S is expected to form a highly porous calcine product (Fig. 1), which has better oxidation kinetics in sulfuric acid solutions than natural pyrrhotite.

Given that a significant portion of the iron can be oxidized to goethite and remain in the leach residue-even at pH 1-using the iron dissolved into solution to calculate the calcine oxidation efficiency does not yield a representative value. Calcine mainly contains quartz and iron sulfides with trace impurities, and quartz is highly thermostable up to 800°C [3]. Therefore, we also developed a sulfur balance analysis method based on the phase transition of iron sulfides to evaluate calcine oxidation.

2. Materials and methods

2.1. Materials and characterization

The mineral phases in the as-received iron-arsenic sulfide concentrate and the calcines were analyzed by X-ray powder diffraction (XRD) using a Philips X'Pert Pro powder diffractometer. Co Kα radiation (λ 1.79 Å) at a step size of 0.02° 2θ and 1.0 s/step was employed. The chemical composition was determined by several methods: atomic absorption spectroscopy for iron concentration; carbon/total sulfur analysis on a CS 200 Carbon/Sulfur machine; thermogravimetry (TGA) in a nitrogen atmosphere with a NETZSCH STA 449 F3 Jupiter® thermal analyzer for S^0 and sulfide content; inductively coupled plasma optical emission spectrometry after aqua regia digestion for other element concentrations; laser particle size analysis; scanning electron microscopy (SEM) to visualize calcine morphology; and automated gas sorption to measure the specific surface area according to the Brunauer-Emmett-Teller theory. The calcine was subjected to density separation to remove the quartz and leave behind mostly pyrrhotite.

In the hydrometallurgical oxidation experiments, 95.0–98.0% sulfuric acid was used to provide the acidic environment, 97% ferric sulfate hydrate (Sigma Aldrich) was a source of Fe^{3+}, and 20 wt.% H_2SO_4 solution or $CaCO_3$ slurry (Powder/Certified ACS; Fisher Chemical) were the pH control agents. To obtain specific particles sizes for some tests, wet grinding was used (see Fig. S2 in Supplementary Material).

2.2. Oxidative leaching tests

Oxidative leaching tests were conducted in a 2-L glass reactor containing 1 L of solution surrounded by a jacketed heater to control the temperature at 95°C under a constant 800 rpm mixing rate (Fig. 2). pH control solutions were added via an Etatron pH/ORP Pump Control System. A pH change of 0.1 triggered the pump system to add H_2SO_4 solution or $CaCO_3$ slurry into the reaction vessel. Tests were conducted in oxidizing conditions with Fe^{3+} and O_2 or O_2 only as oxidants. The oxygen flow rate was constant at 0.5 L/min, and tests were conducted for 48 h.

Solution samples were collected during leaching tests to monitor Fe and As concentrations. After leaching, the final slurry was vacuum filtered. Residues retained on the filter were analyzed for total sulfur content and S speciation distribution (wt.% S^0 and sulfides). Residues for TGA analysis were washed in 15% HCl at 60°C for 1 h to remove metal oxides formed during leaching and then dried in air at 40°C for 24 h. The filtrate (leachate) was analyzed for dissolved Fe and As concentration using atomic absorption spectroscopy. Fe^{2+} concentrations were measured by 0.01 M ceric sulfate titration, based on Eq. (6):

$$Ce^{4+}+Fe^{2+}\ \rightarrow\ Ce^{3+}+Fe^{3+} \quad (6)$$

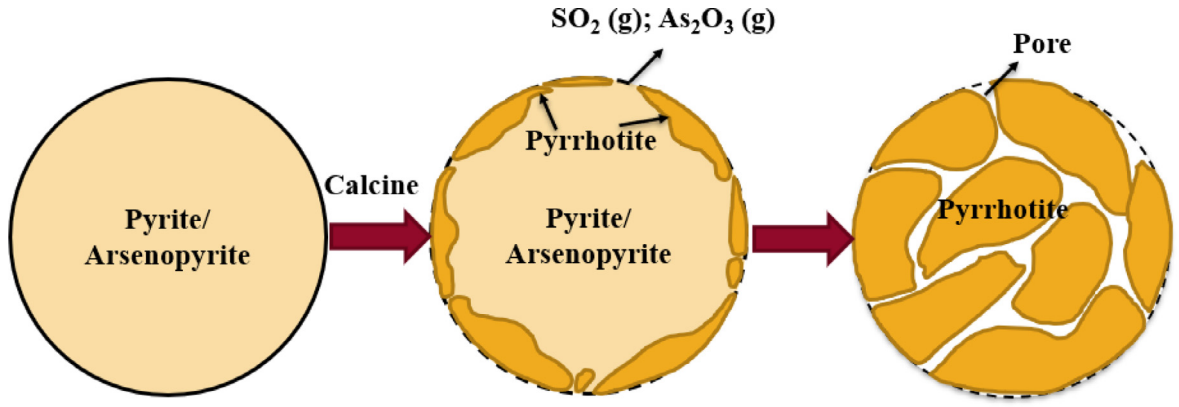

Fig. 1. Schematic of porous pyrrhotite formation from calcination of pyrite/arsenopyrite.

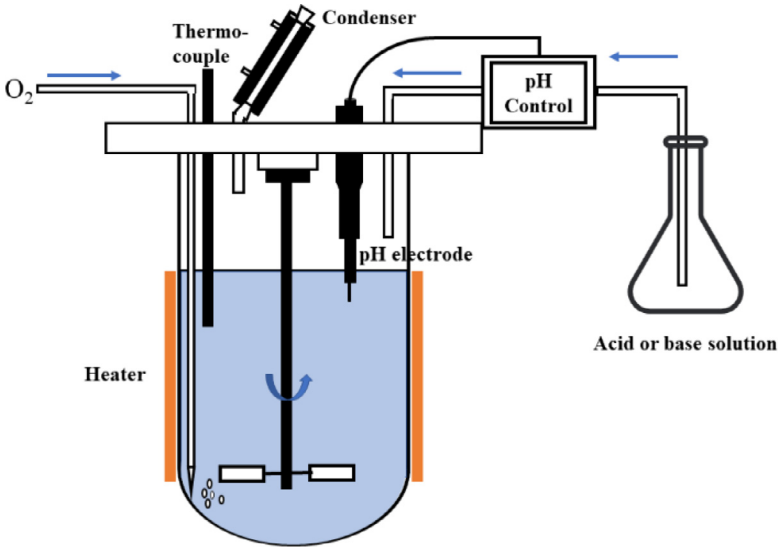

Fig. 2. Schematic of the atmospheric oxidative leaching experimental set-up.

Table 2
Experimental design to test four factors.

Factor	Initial pH	Initial Fe^{3+} (g/L)	Pulp density(% w/v)	Particle size (P80: μm)
Initial pH	1	10	5	36.2
	2	10	5	36.2
	4	0	5	36.2
	5.5	0	5	36.2
Initial Fe^{3+}	1	1	5	36.2
	1	5	5	36.2
	1	10	5	36.2
Pulp density	1	1	5	36.2
	1	1	10	36.2
	1	1	20	36.2
Particle size	1	5	5	32.6
	1	5	5	27.5
	1	5	5	21.8

2.3. Oxidative leaching optimization design

The four factors tested in triplicate oxidative leaching optimization experiments were initial pH, initial Fe^{3+} concentration, pulp density, and particle size (Table 2). Since non-oxidative leaching of pyrrhotite can occur at very low pH and release H_2S, a range of pH values was tested. All designed tests are presented in Supplementary Material (Table S1).

2.4. Sulfur balance analysis and oxidation efficiency calculation

Fe precipitates at near neutral pH, making it impossible to determine the oxidation rate based on the Fe concentration, thus sulfur speciation analysis was required. The weight percentages of S^0 and untreated pyrrhotite were quantified according to the thermal iron sulfide phase transition based on a method using TGA analysis. Pyrrhotite oxidation was calculated by the oxidation percentage of sulfide, relating to the

Table 3
Elemental analysis of the concentrate and the calcine.

Element (wt. %)	As	Al	Ca	Cu	Fe	Ni	S	Si	O
Untreated concentrate	2.60	2.34	1.66	0.22	20.35	0.15	17.65	25.68	29.35
Pyrrhotite calcine	0.21	2.60	1.84	0.24	22.26	0.15	14.70	27.07	30.93

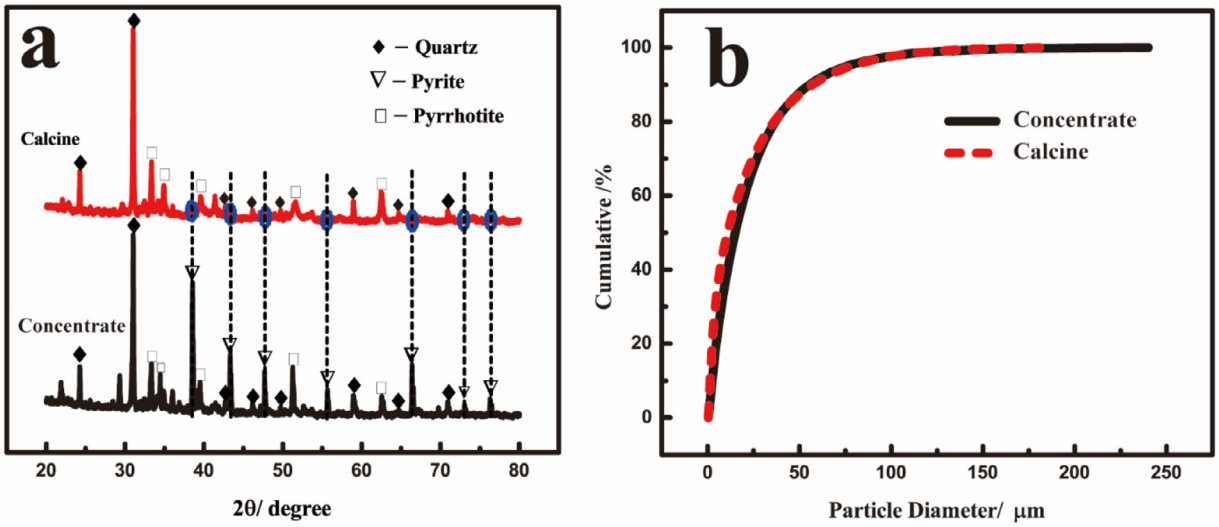

Fig. 3. (a) XRD patterns and (b) particle size distribution of the concentrate and calcine.

sulfur species distribution (elemental sulfur, sulfate, and sulfide) of the final oxidation products.

3. Results and discussion

3.1. Characterization of calcine

Arsenic content was dramatically lower in the calcine than untreated concentrate (Table 3), confirming that the As removal method is highly efficient. The Fe:S molar ratio was higher in the calcine (0.87:1) than concentrate (0.67:1), indicating S loss during calcination.

Based on element analysis (Table 3) and XRD phase analysis (Fig. 3a), the undissolved part of the concentrate and calcine samples after aqua regia digestion was mainly quartz (JCPDS card No. 46-1045) (45.3 and 49.3 wt.%, respectively). Other major phases in the concentrate were pyrite (JCPDS card No. 42–1340) and pyrrhotite (JCPDS card No. 29-0724). The expected arsenopyrite peaks corresponding to 2% As content in the material were absent, nor was pyrite detected in the calcine. Calcination did not change the particle size (Fig. 3b).

Thermal treatment removed As from the concentrate and simultaneously transformed pyrite to pyrrhotite by thermal decomposition, consistent with previous studies showing that pyrolysis of arsenopyrite Eq. (1) and pyrite Eq. (7) yields pyrrhotite as the calcination product [18].

$$FeS_2 = FeS_x(s) + \frac{2-x}{n} S_n(g) \quad (7)$$

where x is between 1 and 2.

Based on the major element (Fe, As, S) contents and excluding quartz and other trace elements, the concentrate and the calcine can be written as $Fe_{0.67}As_{0.06}S$ and $Fe_{0.87}S$, respectively. The iron sulfide content in the calcine is similar to pyrrhotite ($Fe_{0.875}S$), suggesting that the calcine is a mixture of quartz and pyrrhotite. This has been confirmed by studies on the phase transition of iron sulfide minerals (e.g., [5,9]), where the transformation of pyrite to pyrrhotite Eq. (8) occurred between 520 and 650°C [6].

$$FeS_2 = \frac{8}{7} Fe_{0.875}S + \frac{3}{7} S_2 \quad (8)$$

Both calcine and natural pyrrhotite samples contained free and agglomerated submicrometric-sized grains (Fig. 4). However, the porous structure and significant roughness on the calcine (enlarged images in Fig. 4b) are very unlike typical pyrrhotite ore (Fig. 4a) and are thought to be produced during the high-temperature arsenic removal process. The higher specific surface area of calcine (1.46 m^2/g) than natural pyrrhotite (0.97 m^2/g) can greatly influence the oxidative leaching rate by increasing the effective surface area and diffusion of the lixiviant into pores [30]. Therefore, the pyrrhotite generated from calcination should be more amenable to atmospheric oxidative leaching than refractory natural pyrrhotite. The SEM image of untreated concentrate is shown in Fig. S1 in Supplementary Material. Clearly the solid particle size is larger than that of the calcine with more agglomerates. The untreated ore contains significant amount of quartz comparing to the natural pyrrhotite. However, no obvious difference can be found due to the main loss of arsenic and sulfur.

3.2. Oxidative leaching of calcine

3.2.1. Effect of pH

The pH control system maintained the leaching solutions within ± 0.5 V of target pH values (Table 2, Fig. 5a). At low pH, the initial oxidation-reduction potential (ORP) was high and vice versa (Fig. 5b). The Fe^{3+}/Fe^{2+} ratio in the leach solution controls the metal sulfide oxidation reaction. Therefore, when Fe^{3+} existed in the solution at pH 1 and 2, the ORP decreased slightly during the leach (Fig. 5b), which is attributed to pyrrhotite oxidation leading to Fe^{2+} production. At pH 4 and 5, the ORP decreased significantly within 3 h and then remained almost stable.

3.2.1.1. Fe and As concentrations. When O_2 was the oxidant in the solution at pH 4 and 5.5, dissolved Fe concentrations remained very low (Fig. 6a). When 10 g/L Fe^{3+} was the oxidant at pH 1 and 2, the total Fe drastically decreased with leaching time, especially in the first 12 h, such that approximately 31.8 and 14.5%, respectively, remained after 48 h (Fig. 6a). This can be ascribed to the formation of goethite under experimental conditions. The Fe^{3+} concentration strongly depends

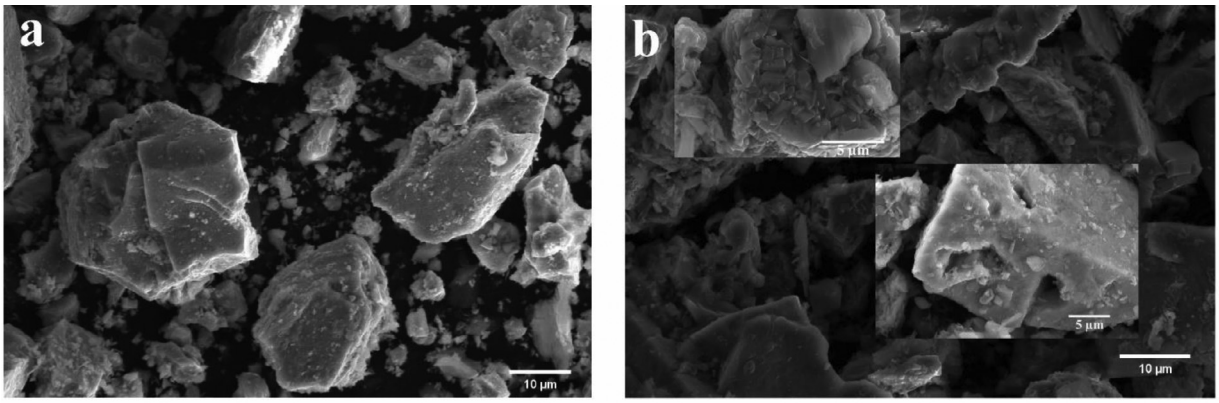

Fig. 4. Scanning electron micrographs of (a) natural pyrrhotite and (b) the calcine.

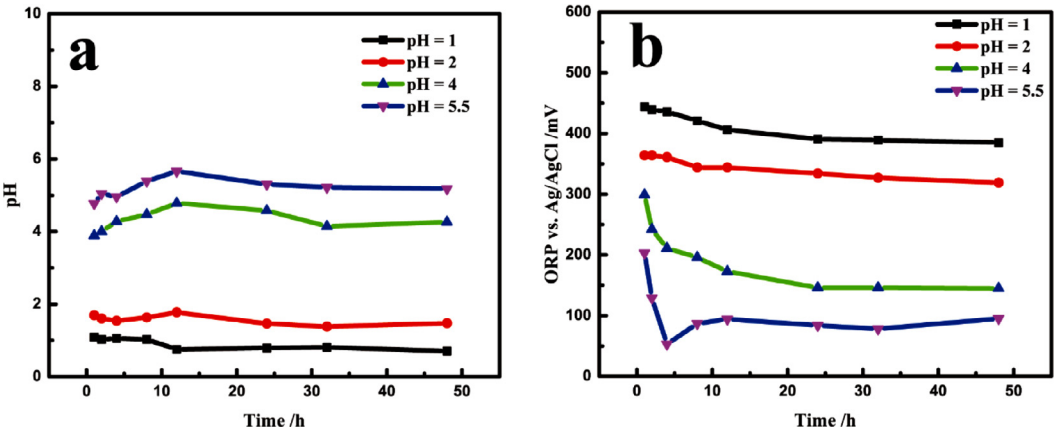

Fig. 5. (a) pH and (b) ORP during calcine oxidative leaching (see Table S1 for test conditions).

on pH and temperature (Fig. 6b): Fe^{3+} begins to precipitate as $Fe(OH)_3$ at pH 2 at 20°C. The two dashed lines in Fig. 6b show that at 95°C, Fe^{3+} is favorably precipitated as goethite at all pH levels tested, even pH 1. Goethite precipitation to remove iron from leach liquor is widely adopted in the industry.

In sulfuric acid solutions at atmospheric pressures, goethite precipitates when iron ions and dissolved oxygen are present Eqs. (9) and ((10).

$$Fe^{3+} + 2\,H_2O = FeOOH + 3\,H^+ \quad (9)$$

$$2\,Fe^{2+} + 0.5\,O_2 + 3H_2O = 2\,FeOOH + 4\,H^+ \quad (10)$$

The Fe^{3+} and Fe^{2+} speciation can further explain the relationship between Fe^{3+} and pyrrhotite. At pH 1, Fe^{2+} concentration increased within 24 h and then slowly decreased and stabilized at 48 h (Fig. 6c), which could be related to more rapid oxidation of Fe^{2+} to Fe^{3+} Eq. (11) than reduction of Fe^{3+} to Fe^{2+} (i.e., pyrrhotite oxidation).

$$2Fe^{2+} + 0.5O_2 + 2H^+ = 2Fe^{3+} + H_2O \quad (11)$$

By comparison, the Fe^{3+} concentration decreased dramatically (Fig. 6c). The disproportionate change in Fe^{3+}/Fe^{2+} concentration caused the decrease in total Fe concentration and Fe^{3+}/Fe^{2+} ratio, which agrees well with the ORP changes in Fig. 5b.

Relative to Fe, dissolved As concentrations in solution were low Fig. 6d). The rapid release of As in the first hour resulted from arsenopyrite oxidation (Eqs. (12) and ((13)).

$$4FeAsS + 11O_2 + 6H_2O \rightarrow 4Fe^{2+} + 4H_3AsO_3 + 4SO_4^{2-} \quad (12)$$

$$2FeAsS + 14Fe^{3+} + 9H_2O \rightarrow 16Fe^{2+} + 2H_3AsO_3 + S_2O_3^{2-} + 12H^+ \quad (13)$$

At pH 1 and 2, As concentrations spiked in the first hour and then dramatically decreased, whereas at higher pH, they did not show a clear spike and decreased slightly or remained stable Fig. 6d). Most likely, the As was initially oxidized to H_3AsO_3 (Eqs. (12) and ((13)) and then further oxidized to As(V) Eqs. (14) and ((15)) [20,21].

$$2\,H_3AsO_3 + O_2 \rightarrow 2H_2AsO_4^- + 2H^+ \quad (14)$$

$$4\,Fe^{2+} + 2O_2 + 4\,H_2AsO_4^{2-} + 4H_2O = 4\left[FeAsO_4 \cdot 2H_2O\right](s) \quad (15)$$

Finally, As(V) likely formed ferric arsenate or scorodite or was absorbed onto the leach residue surface. Goethite and jarosite have been reported as effective As(V) absorbents in highly acidic solutions [2].

3.2.1.2. Sulfur oxidation. Based on studies of iron sulfide pyrolysis in coal, where pyrite and organic sulfur are the two major forms of sulfur [17], pyrite pyrolysis largely determines the distribution of sulfur in solid and gaseous products. Thermal decomposition of pyrite and pyrrhotite can be used as an analytical technique for differentiating the two. Thermal decomposition of pyrite to pyrrhotite begins at 400°C, and pyrrhotite tends to decompose to troilite (FeS) at 600°C [32]. Decomposition of FeS to Fe and S can only occur at temperatures higher than 1,000°C in a N_2 atmosphere [32]. Results of this study showed that pyrrhotite ($Fe_{0.877}S$) is stable at temperatures up to 465°C. At higher temperatures, pyrolysis proceeds to form troilite via Eq. (16) [3].

$$2\,Fe_{1-x}S = 2(1-x)\,FeS + x\,S_2\,(g) \quad (16)$$

In fact, pyrolysis of pyrrhotite in this study in N_2 atmosphere can be written as Eq. (17):

$$Fe_{0.87}S = 0.87\,FeS + 0.065\,S_2\,(g) \quad (17)$$

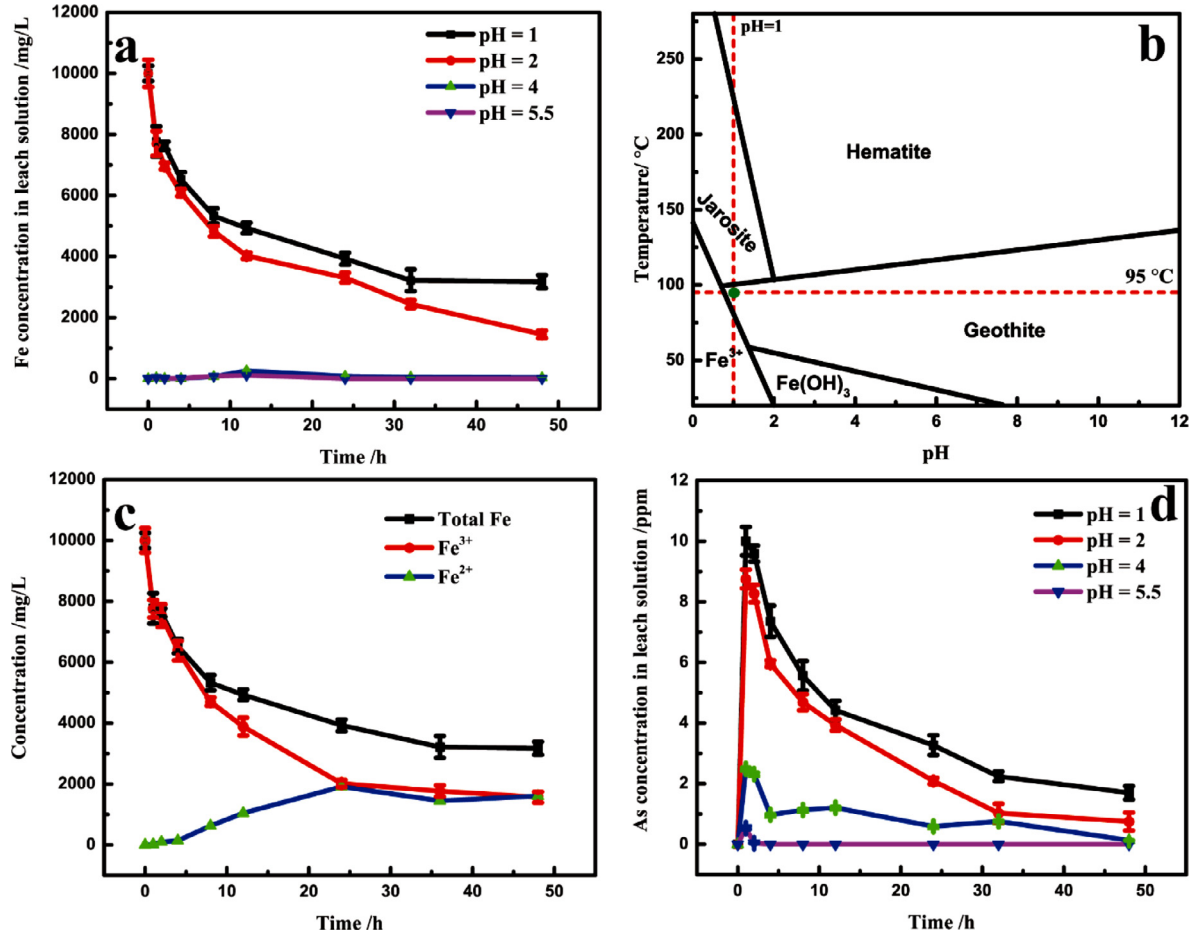

Fig. 6. (a) Total Fe concentration in calcine leaching solution over 48 h at 95°C; (b) predominance area diagram of iron compounds in the Fe-O-H system (modified from [15]); (c) Fe speciation in pH 1 calcine leach solution; (d) As concentration in calcine leaching solution over 48 h at 95°C.

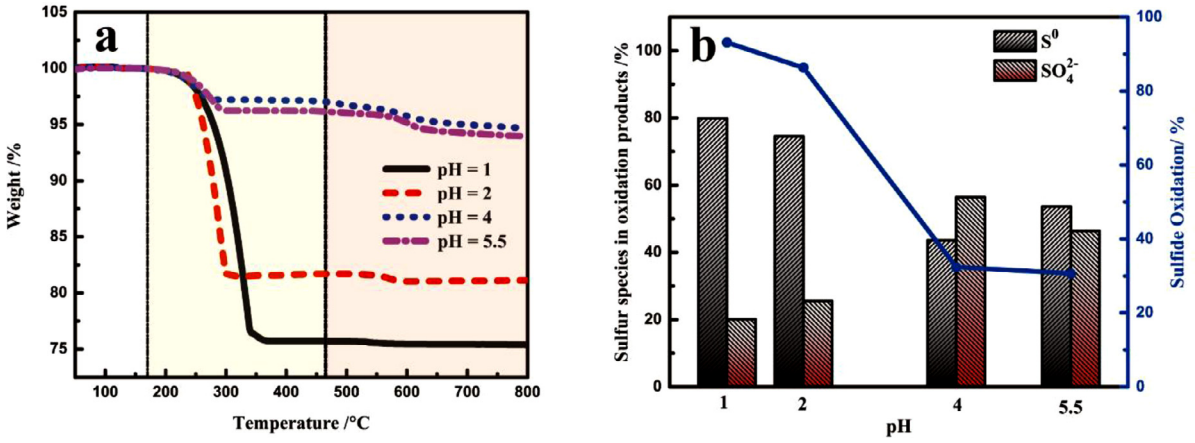

Fig. 7. (a) Thermogravimetric curves of calcine oxidative leaching residues after HCl washing and (b) sulfide oxidation and sulfur speciation as a percentage of total oxidized sulfide in calcine at four pH values.

Using the iron sulfide transformation reaction, the wt.% of unreacted pyrrhotite was calculated from TGA test results in N_2 atmosphere (Fig. 7a). Thus, the oxidative leaching efficiency of the calcine can be determined by S speciation analysis. Sulfur evaporates at 200–350°C. Thus, the sulfur speciation in the residue can also be analyzed. The wt.% of S^0 and unreacted pyrrhotite after HCl leaching in all residues are given in Table S1. The TGA curves of all HCl-washed residues showed two stages of weight loss (Fig. 7b):

1 At temperatures of 170–465°C, S^0 powder was completely removed. More weight loss was observed at pH 1 and 2 (24.3 and 18.3%, respectively) than pH 4 and 5.5 (2.9 and 3.8%, respectively).
2 The unreacted pyrrhotite began to convert to FeS at approximately 465°C and continued until 800°C. Weight loss was negligible at pH 1 and 2 and was 2.9 and 3.8% at pH 4 and 5.5, respectively.

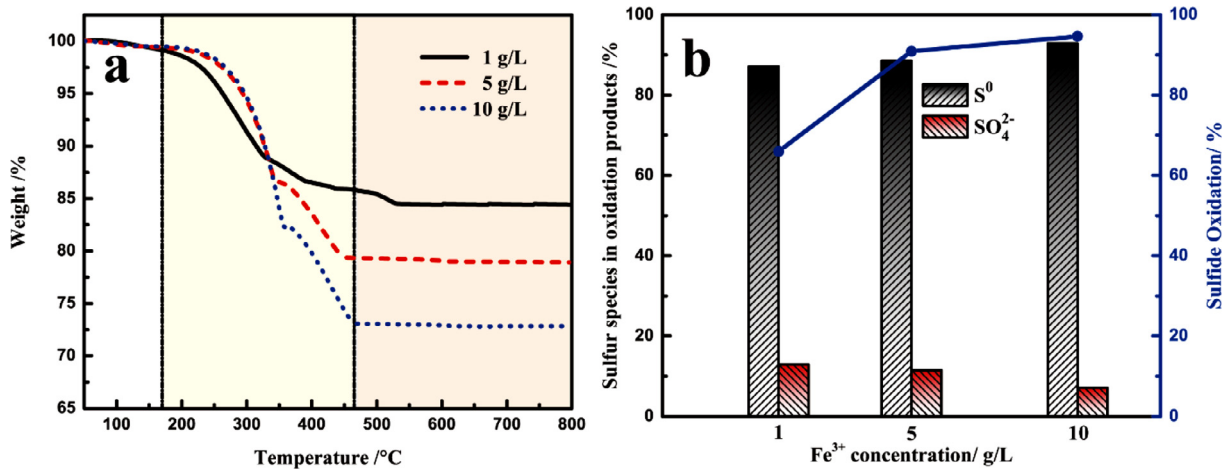

Fig. 8. (a) Thermogravimetric curves of calcine oxidative leaching residues after HCl washing and (b) sulfide oxidation and sulfur speciation as a percentage of total oxidized sulfide in the calcine at three Fe^{3+} concentrations at pH 1.

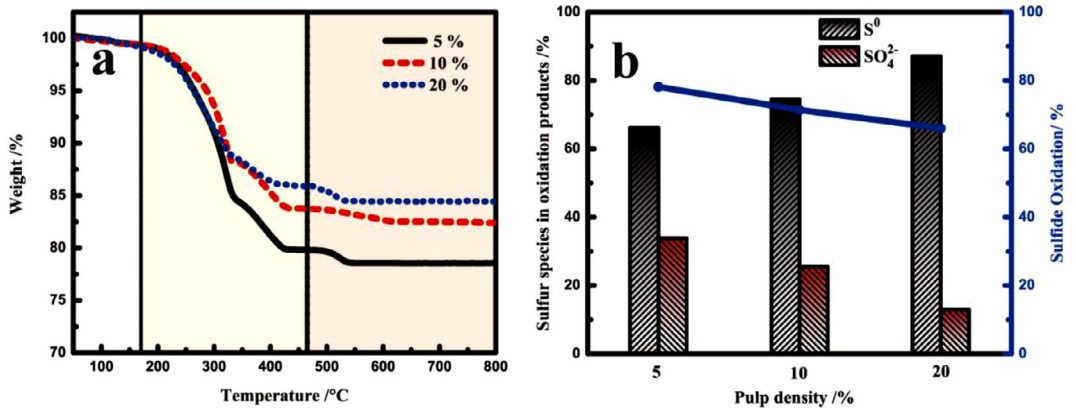

Fig. 9. (a) Thermogravimetric curves of calcine oxidative leaching residues after HCl washing and (b) sulfide oxidation and sulfur speciation as a percentage of total oxidized sulfide in calcine at pH 1, 1 g/L Fe^{3+}, and three initial pulp densities.

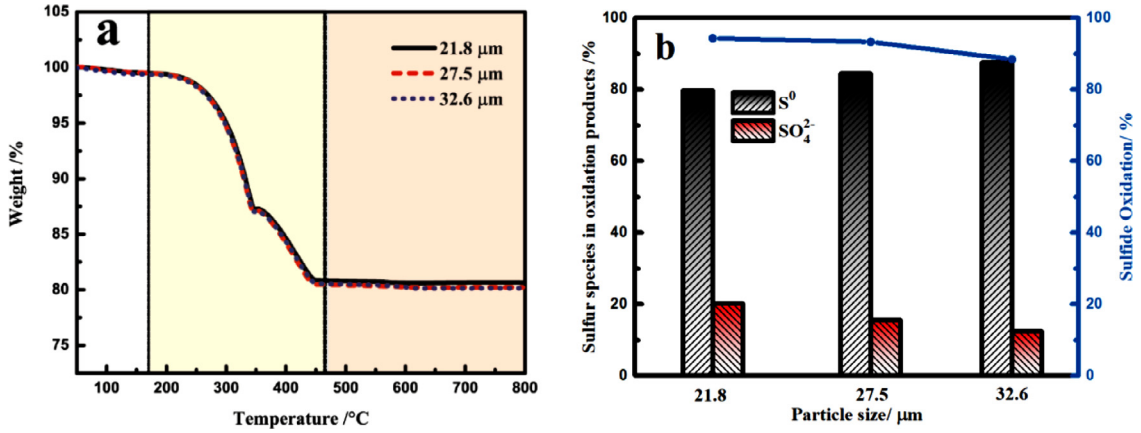

Fig. 10. (a) Thermogravimetric curves of calcine oxidative leaching residues after HCl washing and (b) sulfide oxidation and sulfur speciation as a percentage of total oxidized sulfide in the calcine at pH 1, 5 g/L Fe^{3+}, and three particle sizes.

Calcine oxidation with respect to the sulfur balance can be calculated using Eq. (18).

$$Oxidation\ \% = \frac{S_{total}\% \times Feed - S_2^{2-}\% \times residue}{S_{total}\% \times Feed} \quad (18)$$

The overall pyrrhotite oxidation rate over 48 h decreased with increasing pH (Fig. 7b). At pH 1 and 2 with Fe^{3+} and O_2 as combined oxidants, the oxidative leaching efficiencies were 94.7 and 86.0%, respectively. The major oxidative leaching product was S^0 rather than sulfate (Fig. 7b). At pH 4 and 5.5 with only O_2 as the oxidant, oxidative leaching efficiencies were 32.4 and 30.6%, respectively, and S° constituted only 40–50% of the oxidation products. Therefore, the oxidation mechanisms of Fe^{3+} and O_2 differ.

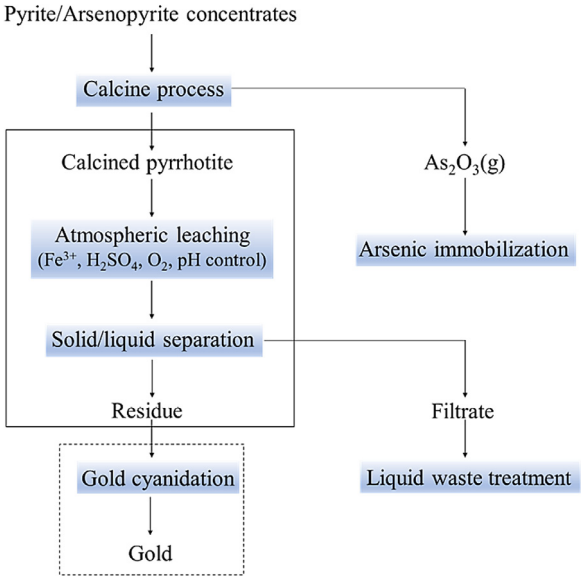

Fig. 11. Flowsheet of gold recovery from pyrite/arsenopyrite calcine.

3.2.2. Effect of initial Fe^{3+} concentration

The effect of Fe^{3+} concentration on calcine oxidative leaching was studied at pH 1. Residues were subjected to TGA analysis and oxidative leaching efficiencies were calculated based on the sulfur balance. In the S evaporation stage (170–465°C) of the TGA test, the obvious inflection point at approximately 350°C (Fig. 8a) is probably related to entrapment of some S^0 in calcine pores that requires more heat and time to escape. Increasing the initial Fe^{3+} concentration produced more S^0 (Fig. 8b), indicating a higher oxidative leaching efficiency pyrrhotite. At 1 g/L Fe^{3+}, lower oxidation efficiency may have resulted from Fe^{3+} precipitation as goethite, making it unavailable for oxidation. Sulfide oxidation was higher at 10 and 5 g/L Fe^{3+} (95 and 91%, respectively) than 1 g/L Fe^{3+} (66%). More than 87% of the oxidation products were S^0, confirming that the dominant oxidation product of calcine at 95°C and pH 1 is S^0.

3.2.3. Effect of initial pulp density

The S^0 wt.% was lower at lower pulp density (Fig. 9a), suggesting that pulp density affects oxidative leaching of calcine. The sulfide oxidation rate decreased with increasing pulp density: at 5% pulp density, 78.0% of the calcine was oxidized, and at 20% pulp density, 67.1% of the calcine was oxidized (Fig. 9b). At the low Fe^{3+} concentration used (1 g/L), maximum pyrrhotite oxidation was not achieved, even at a low pulp density of 5 g/L. By increasing the pulp density from 5 to 20%, the $S^0/SO_4{}^{2-}$ ratio of the oxidation products increased from 2.0 to 6.8 (Fig. 8b).

3.2.4. Effect of particle size

Particle size had little influence on calcine oxidation efficiency. TGA curves showed negligible differences between the three particle sizes (Fig. 10a). The leaching efficiency and main oxidation product (S^0 > 80%) were higher for a smaller particle size (Fig. 10b), but the increase in the oxidation rate was minimal. Since the initial calcine was already very fine (P80 = 36.2 μm), size reduction is not economically beneficial due to the high energy requirements for grinding.

4. Conclusions

This study demonstrated the feasibility of fully oxidizing a calcined product (mainly quartz and pyrrhotite) from a pyrite/arsenopyrite concentrate under atmospheric oxidative leaching conditions. Conventional hydrometallurgical processes to treat refractory pyrrhotite minerals must be conducted at high pressure and temperature to avoid severe passivation from S^0 accumulation on pyrrhotite surfaces at atmospheric pressure conditions. Atmospheric oxidative leaching of the calcined pyrrhotite achieved oxidation rates of > 90%, which is attributed to the high porosity of the calcine after arsenic removal. Theoretically, it is possible that all encapsulated fine gold particles could be released from the iron sulfide hosts due to the high reactivity of the calcined pyrrhotite with a high specific surface area. A sulfur mass balance analysis methodology was developed as a tool to quantify the oxidation efficiency of pyrrhotite. An optimal oxidative leaching efficiency of 95% was achieved at low pH (< 2), 5 g/L Fe^{3+}, 95°C, 800 rpm, O_2 flow rate of 0.5 L/ min, pulp density of 5%, and 48 h reaction time. A significant amount of iron precipitated as goethite. Grinding of the calcine had a negligible effect on oxidative leaching since the initial particle size was fine.

This study provides an efficient oxidative leaching process for calcined pyrrhotite and a promising pre-oxidation process for gold extraction from refractory pyrite/arsenopyrite hosts. Further research will clarify the recovery of the gold by developing a complete flowsheet of gold recovery (Fig. 11).

Declaration of Competing Interest

The authors declare that they have no known competing financial interests or personal relationships that could have appeared to influence the work reported in this paper.

Acknowledgments

The authors are thankful to MITACS and Dundee Sustainable Technologies for financial support to prepare this research article though MITACS Accelerate Fund IT14866. The study benefited from the use of the electron microscope at the RMTL Facility, Queen's University, constructed with funding from the Canada Foundation for Innovation and Ontario Research Fund.

Supplementary materials

Supplementary material associated with this article can be found, in the online version, at doi:10.1016/j.ceja.2021.100122.

References

[1] M.G. Aylmore, Distribution and Agglomeration of Gold in Arsenopyrite and Pyrite. (Doctoral Dissertation, Curtin University, 1995.
[2] A. Basu, M.E. Schreiber, Arsenic release from arsenopyrite weathering: Insights from sequential extraction and microscopic studies, J. Hazard. Mater. 262 (2013) 896–904, doi:10.1016/j.jhazmat.2012.12.027.
[3] R.E. Browner, K.H. Lee, Effect of pyrrhotite reactivity on cyanidation of pyrrhotite produced by pyrolysis of a sulphide ore, Miner. Eng. 11 (1998) 813–820, doi:10.1016/s0892-6875(98)00068-5.
[4] L.J. Cabri, M. Newville, R.A. Gordon, E.D. Crozier, S.R. Sutton, G. McMahon, D.-T. Jiang, Chemical speciation of gold in arsenopyrite, Can. Mineral. 38 (2000) 1265–1281, doi:10.2113/gscanmin.38.5.1265.
[5] H. Chen, B. Li, B. Zhang, Decomposition of pyrite and the interaction of pyrite with coal organic matrix in pyrolysis and hydropyrolysis, Fuel 79 (2000) 1627–1631, doi:10.1016/S0016-2361(00)00015-6.
[6] Y.H. Chen, Y.H. Chen, W.D. Hsu, Y.C. Chang, H.S. Sheu, J.J. Lee, S.K. Lin, Using the high-temperature phase transition of iron sulfide minerals as an indicator of fault slip temperature, Sci. Rep. 9 (2019) 1–6, doi:10.1038/s41598-019-44319-8.
[7] D.H. Cowan, F.G. Jahromi, A. Ghahreman, A parameters study of the novel atmospheric pyrite oxidation process with Lewatit® AF 5 catalyst, Hydrometallurgy 183 (2019) 87–97, doi:10.1016/j.hydromet.2018.11.014.
[8] R. Cruz, I. González, M. Monroy, Electrochemical characterization of pyrrhotite reactivity under simulated weathering conditions, Appl. Geochem. 20 (2005) 109–121, doi:10.1016/j.apgeochem.2004.07.007.
[9] R. Cyprès, M. Ghodsi, R. Stocq, Behaviour of pyrite during hydrogenation of graphite at atmospheric pressure, Fuel 60 (1981) 247–250, doi:10.1016/0016-2361(81)90187-3.
[10] D.J. Droppert, Y. Shang, The leaching behaviour of nickeliferous pyrrhotite concentrate in hot nitric acid, Hydrometallurgy 39 (1995) 169–182 https://doi.org/https://doi.org/, doi:10.1016/0304-386X(95)00034-E.

[11] J.G. Dunn, A.C. Chamberlain, The recovery of gold from refractory arsenopyrite concentrates by pyrolysis-oxidation, Miner. Eng. 10 (1997) 919–928, doi:10.1016/s0892-6875(97)00074-5.
[12] J.G. Dunn, A.S. Ibrado, J. Graham, Pyrolysis of arsenopyrite for gold recovery by cyanidation, Miner. Eng. 8 (1995) 459–471, doi:10.1016/0892-6875(95)00010-N.
[13] V.P. Evangelou, Y.L. Zhang, A review: pyrite oxidation mechanisms and acid mine drainage prevention, Crit. Rev. Environ. Sci. Technol. 25 (1995) 141–199, doi:10.1080/10643389509388477.
[14] D. Filippou, R. Konduru, G.P. Demopoulos, A kinetic study on the acid pressure leaching of pyrrhotite, Hydrometallurgy 47 (1997) 1–18, doi:10.1016/S0304-386X(97)00034-0.
[15] S. Garg, K. Judd, R. Mahadevan, E. Edwards, V.G. Papangelakis, Leaching characteristics of nickeliferous pyrrhotite tailings from the Sudbury, Ontario area, Can. Metall. Q. 56 (2017) 372–381, doi:10.1080/00084433.2017.1361162.
[16] A. Ghahremaninezhad, E. Asselin, D.G. Dixon, In situ electrochemical analysis of surface layers on a pyrrhotite electrode in hydrochloric acid solution, J. Electrochem. Soc. 157 (2010) C248, doi:10.1149/1.3421714.
[17] G. Gryglewicz, P. Wilk, J. Yperman, D.V. Franco, I.I. Maes, J. Mullens, L.C. Van Poucke, Interaction of the organic matrix with pyrite during pyrolysis of a high-sulfur bituminous coal, Fuel 75 (1996) 1499–1504, doi:10.1016/0016-2361(96)00141-X.
[18] D.M. Hausen, Reversible reactions between pyrite and pyrrhotite in SO_2, JOM 43 (1991) 31–34, doi:10.1007/BF03220544.
[19] N. Iglesias, F. Carranza, Refractory gold-bearing ores: a review of treatment methods and recent advances in biotechnological techniques, Hydrometallurgy 34 (1994) 383–395, doi:10.1016/0304-386X(94)90074-4.
[20] F.G. Jahromi, D.H. Cowan, A. Ghahreman, Lanxess Lewatit® AF 5 and activated carbon catalysis of enargite leaching in chloride media; a parameters study, Hydrometallurgy 174 (2017) 184–194 https://doi.org/https://doi.org/, doi:10.1016/j.hydromet.2017.10.012.
[21] F.G. Jahromi, A. Ghahreman, *In-situ* oxidative arsenic precipitation as scorodite during carbon catalyzed enargite leaching process, J. Hazard. Mater. 360 (2018) 631–638 https://doi.org/https://doi.org/, doi:10.1016/j.jhazmat.2018.08.019.
[22] M.P. Janzen, R.V. Nicholson, J.M. Scharer, Pyrrhotite reaction kinetics: Reaction rates for oxidation by oxygen, ferric iron, and for nonoxidative dissolution, Geochim. Cosmochim. Acta 64 (2000) 1511–1522, doi:10.1016/S0016-7037(99)00421-4.
[23] L. Li, I. Bergeron, A. Ghahreman, The effect of temperature on the kinetics of the ferric-ferrous redox couple on pyrite, Electrochim. Acta (2017), doi:10.1016/j.electacta.2017.05.198.
[24] Y. Liu, Z. Dang, Y. Xu, T. Xu, Pyrite passivation by triethylenetetramine: an electrochemical study, J. Anal. Methods Chem. (2013) 2013, doi:10.1155/2013/387124.
[25] L. Maddox, G.M. Bancroft, M.J. Scaini, J.W. Lorimer, Invisible gold: comparison of Au deposition on pyrite and arsenopyrite, Am. Mineral. 83 (1998) 1240–1245, doi:10.2138/am-1998-11-1212.
[26] Y.L. Mikhlin, A.V. Kuklinskiy, N.I. Pavlenko, V.A. Varnek, I.P. Asanov, A.V. Okotrub, G.E. Selyutin, L.A. Solovyev, Spectroscopic and XRD studies of the air degradation of acid-reacted pyrrhotites, Geochim. Cosmochim. Acta 66 (2002) 4057–4067, doi:10.1016/S0016-7037(02)00989-4.
[27] J.R. Mycroft, H.W. Nesbitt, A.R. Pratt, X-ray photoelectron and Auger electron spectroscopy of air-oxidized pyrrhotite: distribution of oxidized species with depth, Geochim. Cosmochim. Acta 59 (1995) 721–733 https://doi.org/https://doi.org/, doi:10.1016/0016-7037(94)00352-M.
[28] A.M. Nazari, R. Radzinski, A. Ghahreman, Review of arsenic metallurgy: treatment of arsenical minerals and the immobilization of arsenic, Hydrometallurgy 174 (2017) 258–281 https://doi.org/https://doi.org/, doi:10.1016/j.hydromet.2016.10.011.
[29] R.V. Nicholson, J.M. Scharer, 1993. Laboratory studies of pyrrhotite oxidation kinetics 14–30. https://doi.org/ 10.1021/bk-1994-0550.ch002
[30] J. Petersen, Heap leaching as a key technology for recovery of values from low-grade ores-a brief overview, Hydrometallurgy 165 (2016) 206–212, doi:10.1016/j.hydromet.2015.09.001.
[31] Z. Tu, C. Guo, T. Zhang, G. Lu, J. Wan, C. Liao, Z. Dang, Investigation of intermediate sulfur species during pyrite oxidation in the presence and absence of acidithiobacillus ferrooxidans, Hydrometallurgy 167 (2017) 58–65, doi:10.1016/j.hydromet.2016.11.001.
[32] A.P. Watkinson, C. Germain, Thermal decomposition of pyrite in fluidized beds, Can. Metall. Q. 11 (1972) 535–547, doi:10.1179/cmq.1972.11.3.535.
[33] M.D. Yuniati, K. Kitagawa, T. Hirajima, H. Miki, N. Okibe, K. Sasaki, Suppression of pyrite oxidation in acid mine drainage by carrier microencapsulation using liquid product of hydrothermal treatment of low-rank coal, and electrochemical behavior of resultant encapsulating coatings, Hydrometallurgy 158 (2015) 83–93, doi:10.1016/j.hydromet.2015.09.028.
[34] Z. Zhao, Y. Zhang, X. Chen, A. Chen, G. Huo, Effect of mechanical activation on the leaching kinetics of pyrrhotite, Hydrometallurgy 99 (2009) 105–108 https://doi.org/https://doi.org/, doi:10.1016/j.hydromet.2009.06.002.